HUMAN COCHLEAR MAPS

Reinhart Frosch
Sommerhaldenstrasse 5B, CH-5200 Brugg, Switzerland; reinifrosch@bluewin.ch
PSI (Paul Scherrer Institute), Villigen and ETH (Eidgenoessische Technische Hochschule), Zurich (retired)

1. INTRODUCTION

In the present context, the term "map" designates a function $x(f)$, where f is the frequency of a sinusoidal tone and x is a related distance from the cochlear base, measured along the cochlear basilar membrane. Presumably, the term "cochlear map" is commonly used because "cochlear function" might be misunderstood as "the way in which the cochlea works". The purpose of cochlear maps is to contribute to a better understanding of cochlear function.

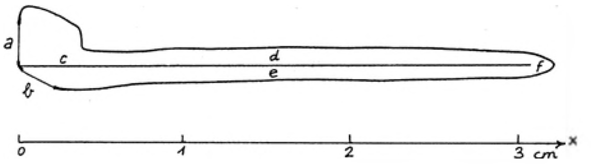

Figure 1. Profile of the unrolled human cochlear channel; a) oval window, b) round window, c) basilar membrane, d) scala vestibuli and scala media (Reissner's membrane is not shown), e) scala tympani, f) helicotrema.

The human cochlea is a liquid-filled helical channel in the temporal bone. An unrolled profile of that channel is shown in Fig. 1. For an adequate description of cochlear physiology, four cochlear-map categories, as specified in Subsections 1.1–1.4, are required. Fig. 41.1 of Frosch (2010a), reproduced in Fig. 2, contains preliminary human cochlear maps. Modified human cochlear maps, first presented in Fig. 4 of Frosch (2010b), are reproduced in Fig. 3. The aim of the present note is to justify that modification.

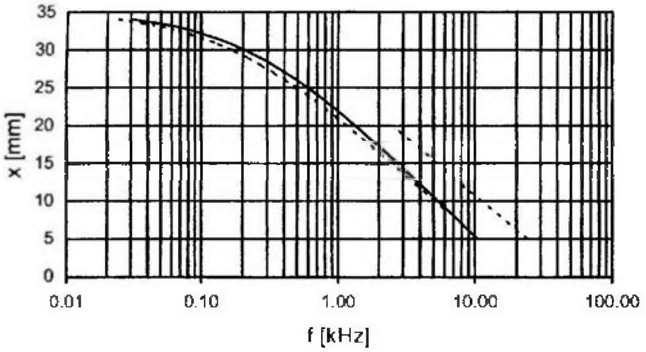

Figure 2. Preliminary human cochlear maps, reproduced from Fig. 41.1 of Frosch (2010a); see text.

1.1 The passive-peak (PP) map

Passive human cochleae (i.e., cochleae in which the mechanical energy generated by active outer hair cells is absent) were studied, e.g., in the post-mortem experiments of von Békésy (1960), who found that during a stationary sinusoidal tone there is a travelling wave in the cochlear channel. In most of those experiments, wave energy was fed into the cochlea through the oval window. That wave energy (kinetic and potential energy of the liquid particles and of the cochlear-partition elements) travels in the $+x$-direction (see Fig. 1). In spite of the fact that this travelling-wave energy starts to be transformed into frictional heat at the cochlear base already, the velocity amplitude of the basilar-membrane (BM) oscillation increases with x. At the passive-peak place $x_{\mathrm{PP}}(f)$, that increase stops, and at greater x the amplitude quickly drops to small values. At high [low] f, $x_{\mathrm{PP}}(f)$ is small [large], as shown in Fig. 2, where $x_{\mathrm{PP}}(f)$ is given by the lower dashed curve, ranging from 0.025 to 6 kHz.

1.2 The low-level active-peak (AP) map

At high f and low sound-pressure level (SPL), the active BM oscillation velocity peak can be much higher and sharper than the just described passive peak. The active peak arises because in a healthy cochlea the outer hair cells (OHCs) near $x_{\mathrm{PP}}(f)$ feed mechanical energy into the cochlear travelling wave. The AP-map place $x_{\mathrm{AP}}(f)$, shown by the solid curve in Fig. 2, is defined to be the active-peak place in a healthy cochlea at SPL < 20dB. The maximal power that healthy OHCs can feed into cochlear travelling waves is so small that its influence on the place of maximal BM oscillation velocity is negligible at SPL > 100dB; i.e., above 100 dB the BM oscillation velocity peak is close to the passive peak even in a healthy cochlea.

1.3 The basilar-membrane resonator (BMR) map

That map, i.e., the function $x_{\mathrm{BMR}}(f)$, shown in Fig. 2 by the upper dashed curve, ranging from 2.5 to 24 kHz, gives the place of that organ-of-Corti slice (BM element and attached cells) which in a cochlea without liquid above and below the partition would have a free-oscillation frequency of f. During the oscillations of the BM resonator, the center-of-mass of the considered organ-of-Corti slice oscillates in a direction perpendicular to the BM. A detailed discussion of the BMR map is given in Chapter 34 of Frosch (2010a).

1.4 The internal organ-of-Corti resonator (IOCR) map

The IOCR-map $x_{\mathrm{IOCR}}(f)$, similarly to the BMR map, defines the place of that element of the internal organ-of-Corti (IOC) resonator which in a cochlea without liquid above and below the partition would have a free-oscillation frequency of f. During the oscillations of the IOC resonator, the *shape* of the considered organ-of-Corti slice varies periodically. As discussed in Chapter 41 of Frosch (2010a), the human IOCR map is conjectured to coincide, for $f > 1$ kHz, with the PP map (lower dashed curve). The IOC resonator enables the outer hair cells to feed energy into cochlear travelling waves and thus to give rise to the active BM oscillation velocity peak. The main source of that energy is conjectured to be the electric current which flows through the outer hair cells and is modulated by the stereocilia of those cells.

2. THE MAPS OF FROSCH (2010a)

These preliminary human cochlear maps are shown in Fig. 2 above. The lower dotted curve (0.025–6 kHz) is taken from Fig. 1 of Greenwood (1990); that Greenwood map, predominantly based on post-mortem measurements, is conjectured to be close to the passive-peak (PP) map.

I have not found published direct experimental determinations of the human active-peak (AP) map. The solid curve in Fig. 2 (0.03–10 kHz) is the result of an attempt to derive the AP map indirectly from published results of psychoacoustic experiments; see Chapter 41 of Frosch (2010a). Briefly, Eq. (10.29) and Fig. 10.10 of Hartmann (1998) yield the “Cambridge” critical-band number $z(f)$; for instance, $z(0) = 0$, and $z(20\text{kHz}) = 41.5$. The solid curve in Fig. 2 is based on the assumption that the function $x(z)$ is exactly linear [Eq. (41.3) of Frosch (2010a)]; e.g., $x(z=0) = 35\text{mm}$, and $x(z=41.5) = 0$. As stated in Frosch (2010a), the just mentioned assumption, and therefore the AP-map curve in Fig. 2 above, cannot be claimed to be accurate.

3. THE MAPS OF FROSCH (2010b)

Thanks to in-vivo experiments, the cochlear maps of several mammals are known better than those of humans; see Chapters 38 (guinea-pig), 39 (chinchilla), and 40 (Mongolian gerbil) in Frosch (2010a). These mammalian maps are similar to those in Fig. 2; the mammalian active-peak (AP) map curves at small x, however, are about halfway between the PP and the BMR map curves, so that at given (small) x the AP-map frequency $f_{\text{AP}}(x)$ is higher, by half an octave, than $f_{\text{PP}}(x)$. The corresponding half-octave difference between $f_{\text{IOCR}}(x)$ [which is postulated to be close to $f_{\text{PP}}(x)$] and $f_{\text{AP}}(x)$ is plausible, since the (–10dB) width of the IOCR resonance peak amounts to about one octave; the mentioned half-octave frequency difference implies that the low-level active BM-oscillation velocity peak is located at the large-x limit of the zone of the strongly active outer hair cells.

The modified human cochlear maps, represented in Fig.3, are based on the hypothesis that the human maps resemble those of the mentioned mammals; in particular, the AP-map frequency $f_{\text{AP}}(x)$ is assumed to be higher by half an octave than $f_{\text{IOCR}}(x)$. The PP-map in Fig. 3 is intended to range from 0.025 to 6 kHz; the IOCR-map is postulated to coincide with the PP-map, but to range from 1 to 6 kHz only. At frequencies to the left and to the right of the curves in Fig. 3 the maps are concluded to be not yet known.

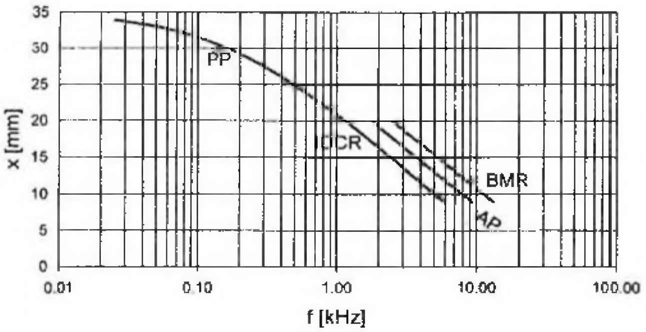

Figure 3. Modified human cochlear maps, reproduced from Fig. 4 of Frosch (2010b); see text.

4. CONCLUSIONS

In the modified human-map diagram (Fig. 3) the active-peak (AP) map, giving the location of the basilar-membrane oscillation velocity peak generated in a healthy cochlea by a sinusoidal tone of low sound-pressure level, differs from that in the previously published diagram (Fig. 2). That change is based on the hypothesis that the cochlear physiology of humans closely resembles that of guinea-pigs, chinchillas, and Mongolian gerbils.

REFERENCES

Von Békésy, G. (1960). Experiments in Hearing. McGraw-Hill, New York, pp. 403-484.

Frosch, R. (2010a). Introduction to Cochlear Waves. vdf, Zurich, pp. 331-386.

Frosch, R. (2010b). Analysis of Human Oto-Acoustic Emissions. Canadian Acoustics, Vol.38, No.3, 88-89.

Greenwood, D.D. (1990). A cochlear frequency-position function for several species – 29 years later. J. Acoust. Soc. Am. 87, 2592-2605.

Hartmann, W.M. (1998). Signals, Sound, and Sensation. Springer, New York, pp. 251, 253.